Observation of cavity polaritons in a metal-mirror Fabry-Pérot microcavity containing liquid-crystalline semiconductor based on perylene bisimide units

Nobutaka Kani, Makoto Suzuki, Kouichi Nishiyama, Shunsuke Nakanishi, Masahiro Funahashi, and Noriaki Tsurumachi[*]

Faculty of Engineering and Design, Kagawa University, 2217-20 Hayashi-cho, Takamatsu 761-0396, Japan

We investigate the optical properties of a metal-mirror microcavity containing a liquid-crystalline (LC) perylene tetracarboxylic bisimide (PTCBI) derivative. Measurements of the transmission's incidence angle dependence show that the peaks are split in a complex way and shift as the angle changes. Further, measurements of the photoluminescence spectrum's emission angle dependence show that the peak also shifts with the angle, as in the transmission experiment. We also carry out a theoretical analysis; the theoretical and experimental results are in very good agreement, and we estimate the vacuum Rabi splitting energies to be about 212, 180, and 240 meV. In addition, the peak photoluminescence energy coincides with the lower polariton branch obtained by transmission experiment. Finally, in a time-resolved photoluminescence experiment, we observe a fast relaxation component that is not seen in the bare LC PTCBI film. We believe this is due to cavity effects increasing the spontaneous emission transition rate, indicating that the emissions are due to cavity polaritons.

I. INTRODUCTION

Traditionally, the interactions between photons and matter in microcavities have been divided into weak and strong coupling regimes depending on their strength [1], but, in recent years, the concept of ultrastrong coupling has also emerged [2]. In the strong coupling regime, strong interactions between atoms or excitons and photons generate hybrid modes known as cavity polaritons. When this occurs, the microcavity's optical modes split into two. This is known as vacuum Rabi splitting, and its magnitude is known to depend on the microcavity's mode volume and the oscillator strength of the matter [3]. Organic materials have received particular attention, due to their large oscillator strength. Cavity polaritons have already been observed in various organic systems, such as cyanine J aggregates [4–6], polymers [7], and single crystals [8]. Furthermore, in recent years, cavity polaritons with very large vacuum Rabi splitting energies (above 1 eV) have been observed using squaraine crystals, and an ultrastrong coupling state has even been realized [9].

Organic semiconductors have several advantages for use in practical devices, such as ease of fabrication and light weight, as well as large oscillator strength. In addition, since they are formed by the van der Waals forces between molecules, the resulting structures have very high degrees of freedom and are highly flexible. Due to having such excellent properties, they have been applied in a range of research fields, such as solar cells [10], field-effect transistors [11], and organic electroluminescence devices [12].

That said, however, organic devices also face many significant problems, such as low device durability, difficulty in controlling the molecular orientation, and difficulty in achieving both carrier mobility and solubility in a given solvent. Controlling the molecular orientations is considered to be a particularly serious issue, since the characteristics of organic semiconductor-based devices are strongly affected by the arrangement of the molecules.

Liquid-crystalline (LC) materials [13] have been proposed as a way to solve these problems. These have the advantage that high-quality films with regularly ordered molecules can be created even by the types of inexpensive and simple solution processes used for thin polymer films. There are many types of LC organic semiconductors with excellent electrical properties, such as high carrier mobility [14–16] and ferroelectricity [17,18], as well as optical properties such as high-quantum-efficiency light emission [19–21] and production of circularly polarized light by introducing chirality [22–24]. Therefore, investigating the cavity quantum electrodynamic properties of such systems is a promising route to future applications.

We have also focused on such LC organic semiconductors, and have succeeded in using them to achieve strong coupling in one-dimensional photonic crystal (1DPC) microcavities [25]. We have also observed polarization anisotropy caused by their self-organization affecting the molecular orientations, as well as relatively large vacuum Rabi splitting (up to 189 meV). However, despite the advantages of our 1DPC microcavities, such as no absorption loss in the mirror component, they also had several drawbacks. First, the mode volume was relatively large, due to the light bleeding peculiar to their dielectric multilayer film structure. Second, the microcavity's stop band (photonic band gap) was narrower than the width of the absorption spectrum of the LC organic semiconductor, meaning that it was not possible to create strong coupling between all transition states of the LC organic semiconductor that we used and the light when using typical materials, such as SiO_2 or TiO_2, for the multilayer mirrors.

To address these problems, in this paper, we adopt a metal-mirror-type Fabry-Pérot microcavity that both enables the

———————
[*]Corresponding author: tsuru@eng.kagawa-u.ac.jp
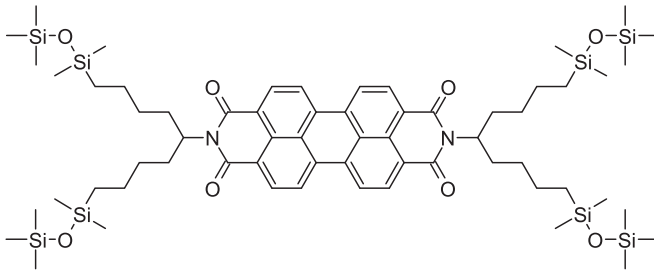
FIG. 1. Chemical structure of PTCBI with four 1,1,1,3,3-pentamethyldisiloxane chains.

FIG. 2. Absorption spectrum (solid line) and photoluminescence spectrum (dashed line) of the LC PTCBI film at room temperature.

mode volume to be extremely small and allows a wide mode splitting range to be observed. By introducing LC organic semiconductors, we aim to observe cavity polaritons with larger vacuum Rabi splitting energies. In addition, we also investigate the microcavity's photoluminescence properties, in order to clarify the organic cavity polariton's relaxation process.

II. EXPERIMENTAL PROCEDURE

In this paper, we utilized a LC perylene tetracarboxylic bisimide (PTCBI) bearing four 1,1,1,3,3-pentamethyldisiloxane chains [26], as shown in Fig. 1. Unlike conventional columnar LCs bearing alkyl side chains, this compound is characterized by bulky organoligosiloxane side chains. At room temperature, it exhibits a rectangular columnar ordered phase. The disiloxane chains make it possible to inhibit close molecular packing (crystallization) and to maintain its LC properties even at low temperatures by adjusting the molecular spacing. Moreover, the side chains also improve its solubility in a solvent.

Despite the presence of these bulky substituents, one-dimensional columnar aggregates with periodically stacked perylene bisimide cores are formed in the columnar phase via nanosegregation between the crystal-like π stacks and liquidlike disiloxane moieties [26]. This means that the electron mobility at room temperature is also very high for an organic semiconductor, at 10^{-1} cm^2/V s. Previously, we have successfully observed cavity polaritons using this PTCBI derivative [25].

Next, we explain how the metal-mirror microcavity used in this paper was fabricated. First, a 28.5-mM chloroform solution of the PTCBI derivative was prepared. Then, this solution was dropped onto a metal mirror, prepared by creating a thin silver film (30-nm average thickness) via vacuum evaporation on a glass slide substrate and spin coating at 4000 rpm for 10 s. Then, another thin silver film (also 30 nm thick) was deposited onto the PTCBI film by vacuum evaporation to form a Fabry-Pérot microcavity.

After that, the transmission spectra of the resulting microcavity were measured, using a halogen lamp light source and a multichannel spectrophotometer (USB 2000, Ocean Optics) at incidence angles of 0°–50°, in steps of 2°. The resonant mode can be tuned by changing the incident angle of light to the microcavity.

Next, the photoluminescence spectra and luminescence lifetime were measured. The excitation light source used was
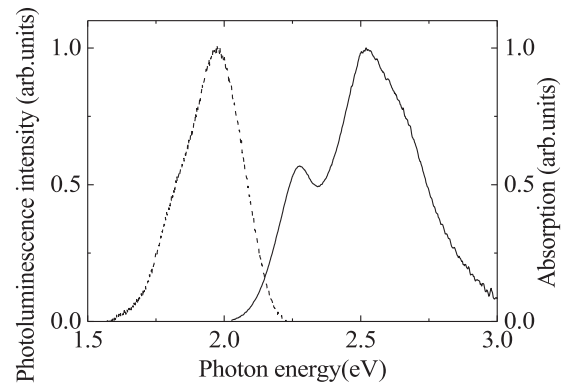
a picosecond pulse laser (PiL040, Advanced Laser Diode Systems) with a repetition frequency of 1 MHz, a central wavelength of 403 nm, and a power of 0.1 mW. The resulting luminescence was detected by a digital charge-coupled device camera (C9300, Hamamatsu Photonics), using a spectrometer (C11119, Hamamatsu Photonics) to resolve the wavelength and a streak scope (C10627, Hamamatsu Photonics) to resolve the time. Here, the emissions were measured at angles of 0°–50° from the direction perpendicular to the sample surface, in steps of 10°.

III. RESULTS AND DISCUSSION

The normalized absorption and photoluminescence spectra for the thin LC PTCBI film are shown in Fig. 2. Here, the solid and dashed lines are the absorption and photoluminescence spectra, respectively. We can observe three absorption peaks, at 2.27 eV (547 nm), 2.52 eV (496 nm), and 2.67 eV (464 nm), and one luminescence peak at 1.97 eV (628 nm), which are determined by multi-Gaussian fitting. We attribute these absorption peaks to the PTCBI's vibronic states, meaning that cavity photons can be strongly coupled to these multiple vibronic transitions [27].

Figure 3 shows the dependence of the microcavity's transmission spectrum on the incident angle. This gives spectra at
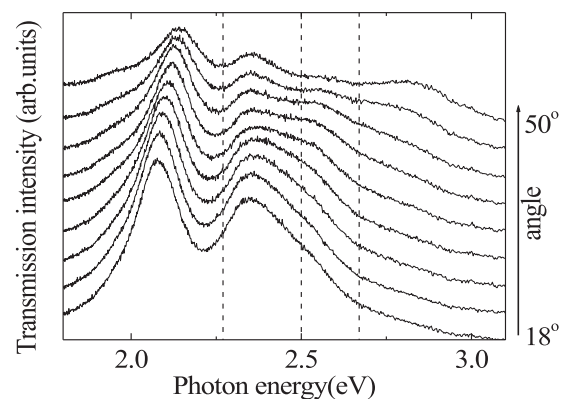

FIG. 3. Dependence of the transmission spectrum on the incidence angle (solid lines). The dotted lines show the peak absorption energies of a bare LC PTCBI thin film.
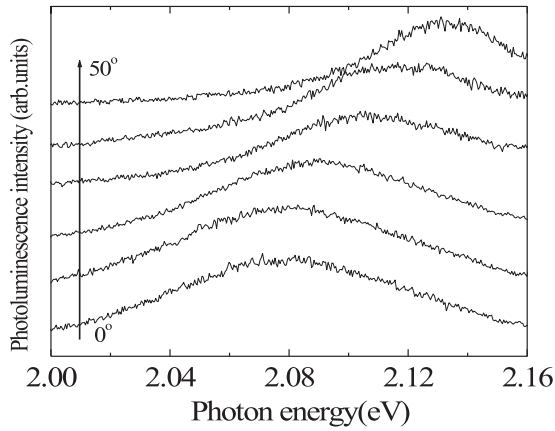
FIG. 4. Dependence of the photoluminescence spectrum (solid lines) on the emission angle.

angles of 18°–50° in steps of 4°, with the solid and dotted lines indicating the transmission spectra and a bare LC PTCBI thin film's peak absorption energies, respectively. Here, we can see that the peaks are split in complex ways and shift as the angle changes.

Next, Fig. 4 shows the dependence of the microcavity's photoluminescence spectrum on the emission angle, at angles of 0°–50° in steps of 10°. These results are normalized by the intensity of each peak. As with the transmission experiment above, the peak shifts with the angle. By contrast, for the bare thin film, neither the absorption nor the emissions depend on the angle. In addition, the microcavity's photoluminescence peak energies are lower than those of the bare film.

Figure 5 plots the energies of the transmission peaks (open circles) and photoluminescence peaks (closed circles) as a function of angle. We obtained the peak value of the transmission spectrum, which was determined by finding out the maximum value in the range between each vibronic level deduced from the absorption spectrum of naked liquid-crystalline thin film. Therefore, we did not estimate the maximum value in the range where the transmission intensity was low and the signal-to-noise ratio was poor. We also analyzed this process

theoretically using a coupled harmonic oscillator Hamiltonian. For the coupling of single-state excitons and photons in the cavity, the two energy eigenvalues of the cavity polariton [the upper polariton branch and the lower polariton (LP) branch] are obtained by substituting a Hamiltonian represented by a 2 × 2 matrix into the Schrödinger equation in general. Since this LC PTCBI film has three vibronic modes, the corresponding Hamiltonian [27–29] is a 4 × 4 matrix as follows:

$$H = \begin{pmatrix} E_{ph} & \Delta E_1^{Rabi}/2 & \Delta E_2^{Rabi}/2 & \Delta E_3^{Rabi}/2 \\ \Delta E_1^{Rabi}/2 & E_{ex1} & 0 & 0 \\ \Delta E_2^{Rabi}/2 & 0 & E_{ex2} & 0 \\ \Delta E_3^{Rabi}/2 & 0 & 0 & E_{ex3} \end{pmatrix}. \tag{1}$$

Here, E_{ex1}, E_{ex2}, and E_{ex3} are the film's transition energies, and ΔE_1^{Rabi}, ΔE_2^{Rabi}, and ΔE_3^{Rabi} are the corresponding vacuum Rabi splitting energies. In addition, E_{ph} is the microcavity's resonance energy as a function of the incidence angle θ when we ignore interactions between the photons and the vibronic states, and is given by

$$E_{ph}(\theta) = E_0 \left(1 - \frac{\sin^2\theta}{n^2} \right)^{-\frac{1}{2}}. \tag{2}$$

Here, n and E_0 are the cavity layer's effective refractive index and the microcavity's resonance energy at an incidence angle of 0°, respectively.

An analysis using this Hamiltonian yields four energy eigenvalues, corresponding to the LP, middle polariton 1, middle polariton 2, and upper polariton [27]. Figure 5 shows that the resulting dispersion relations (solid lines) are in very good agreement with the experimental results.

In addition, we estimated the vacuum Rabi splitting energies ΔE_1^{Rabi}, ΔE_2^{Rabi}, and ΔE_3^{Rabi} to be about 212, 180, and 240 meV, respectively, or about 9.4, 7.2, and 9.0% of the vibronic transition energies. The ultrastrong coupling
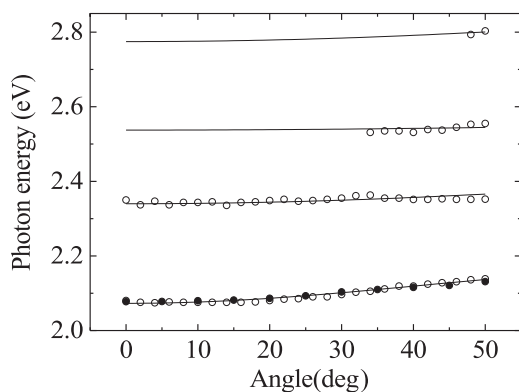

FIG. 5. Dispersion curves for the cavity polaritons, calculated using the coupled harmonic oscillator Hamiltonian (solid lines). The open and closed circles plot the energies of the transmission and photoluminescence peaks, respectively, as a function of angle.
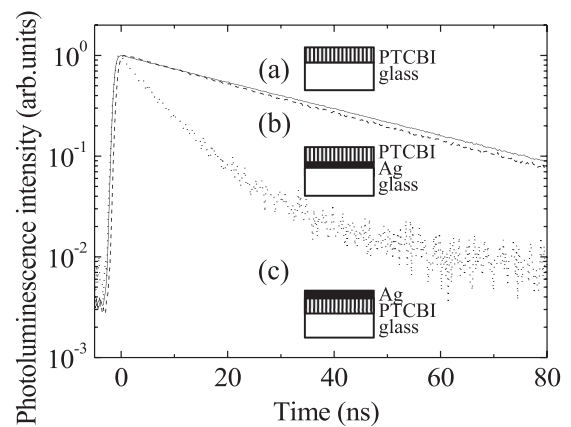

FIG. 6. Photoluminescence decay curves of three types of thin LC PTCBI films, namely, (a) a thin PTCBI film spin coated onto a glass substrate (solid line), (b) a thin silver film deposited onto a glass substrate and then spin coated with a thin PTCBI film (broken line), and (c) a thin silver film deposited on a thin spin-coated PTCBI film on a substrate (dotted line).
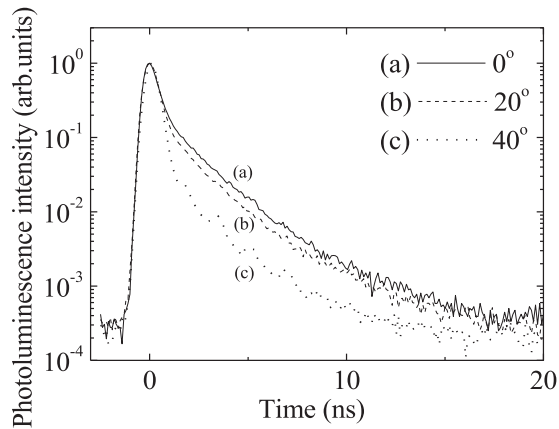
FIG. 7. Photoluminescence decay curves of the microcavity structure, at emission angles of (a) 0° (solid line), (b) 20° (broken line), and (c) 40° (dotted line).

regime is characterized by splitting energies exceeding 20% of the transition energy [2], so our system did not produce ultrastrong coupling states. However, the coupling is nonetheless stronger than that we previously obtained with a 1DPC microcavity [25], which we believe is due to the switch from multilayer dielectrics to a metal-mirror microcavity resulting in a smaller mode volume. In addition, the photoluminescence peak energy coincides with the LP branch obtained in the transmission experiment above.

Next, we discuss the time-resolved photoluminescence. Figure 6 shows photoluminescence decay curves for three types of thin LC PTCBI films, namely, (a) a spin-coated PTCBI thin film on a glass substrate (solid line), (b) a thin silver film deposited on a glass substrate and then spin coated with a thin PTCBI film (broken line), and (c) a thin silver film deposited on a spin-coated thin PTCBI film on a substrate (dotted line). Although none of these films have a cavity structure, the thin silver films were created under the same conditions used to fabricate the microcavity and were about 30 nm thick.

Figures 6(a) and 6(b) show single exponential decay curves, while Fig. 6(c) shows biexponential decay. Based on these results, we estimated the emission lifetimes to be (a) 33 ns, (b) 30 ns, and (c) 6.3 and 32.7 ns. In Fig. 6(c), where silver was deposited onto a thin PTCBI film, there were two types of molecules, namely, those that were quenched by direct contact with the silver and those that were not in contact with the silver and thus exhibited normal luminescence, and we believe this is why there were two relaxation components. These results are for a 0° emission angle, and essentially the same results were obtained at all other angles.

The experimental results of time-resolved photoluminescence of the microcavity structure are shown in Fig. 7, at emission angles of (a) 0° (solid line), (b) 20° (broken line),

and (c) 40° (dotted line). These curves can all be fitted with three exponential decay components, and the time constants at 0° are $\tau_1 = 470$ ps, $\tau_2 = 2.1$ ns, and $\tau_3 = 32.7$ ns. The slowest component (τ_3) is intrinsic to the thin PTCBI film and is almost the same as that obtained in Fig. 6. The next slowest component is probably due to the molecules affected by metal quenching. We believe that the metal quenching effect is stronger for this sample than for the thin film in Fig. 6 due to there being silver layers both above and below the LC PTCBI layer and the fact that this film is thinner. Finally, we believe the fastest component is due to cavity effects increasing the spontaneous emission transition rate. The proportion of this component increases with the emission angle and is largest at around 40°, where the lowest-order vibronic mode coincides with the cavity photon mode. Thus, we consider that the larger the emission angle the more it is influenced by the cavity [30]. As discussed above, we can see that the light emission process reflects the properties of the cavity polaritons.

IV. CONCLUSION

Building on our previous study of cavity quantum electrodynamic effects in LC PTCBI derivatives in the 1DPC microcavities, we have successfully observed cavity polaritons that exhibit larger Rabi splitting with a Fabry-Pérot microcavity that used metal mirrors to achieve a smaller mode volume. We were also able to observe Rabi splitting for all vibronic transitions in LC PTCBI derivatives thanks to the metal-mirror microcavity's broader stop band, estimating the vacuum Rabi splitting energies to be about 212, 180, and 240 meV, respectively. Since these results represent around 9.4, 7.2, and 9.0% of the vibronic transition energies, respectively, they do not represent ultrastrong coupling states, but they are nonetheless higher than those previously obtained for the 1DPC microcavity. In addition, the photoluminescence peak energy coincided with the LP branch obtained in our transmission experiment. Finally, in our time-resolved photoluminescence experiment, we observed a fast relaxation component that was not seen in the bare PTCBI LC film. This is considered to be the increase in the spontaneous emission transition rate due to a cavity effect, indicating that these emissions are due to cavity polaritons.

[1] A. V. Kavokin, J. J. Baumberg, G. Malpuech, and F. P. Laussy, *Microcavities* (Oxford University, New York, 2007).

[2] A. F. Kockum, A. Miranowicz, S. De Loberato, S. Savasta, and F. Nori, Nat. Rev. Phys. **1**, 19 (2019).

[3] M. Fox, *Quantum Optics* (Oxford University, New York, 2006), Chap. 10, p. 208.

[4] D. G. Lidzey, D. D. C. Bradley, T. Virgili, A. Armitage, M. S. Skolnick, and S. Walker, Phys. Rev. Lett. **82**, 3316 (1999).

[5] M. Oda, K. Hirata, T. Inoue, Y. Obara, T. Fujimura, and T. Tani, Phys. Status Solidi C **6**, 288 (2009).

[6] K. Ishii, S. Nakanishi, and N. Tsurumachi, Appl. Phys. Lett. **103**, 013301 (2013).

[7] R. F. Oulton, N. Takada, J. Koe, P. N. Stavrinou, and D. D. C. Bradley, Semicond. Sci. Technol. **18**, S419 (2003).

[8] H. Kondo, Y. Yamamoto, A. Takeda, S. Yamamoto, and H. Kurisu, J. Lumin. **128**, 777 (2008).

[9] S. Gambino, M. Mazzeo, A. Genco, O. Di Stefano, S. Savasta, S. Patanè, D. Ballarini, F. Mangione, G. Lerario, D. Sanvitto, and G. Gigli, ACS Photonics **1**, 1042 (2014).

[10] S. Günes, H. Neugebauer, and N. S. Sariciftci, Chem. Rev. **107**, 1324 (2007).

[11] Y. Guo, G. Yu, and Y. Liu, Adv. Mater. **22**, 4427 (2010).

[12] A. C. Grimsdale, K. L. Chan, R. E. Martin, P. G. Jokisz, and A. B. Holmes, Chem. Rev. **109**, 897 (2009).

[13] M. Funahashi, J. Mater. Chem. C **2**, 7451 (2014).

[14] M. Funahashi, Polym. J. **41**, 459 (2009).

[15] M. O'Neill and S. M. Kelly, Adv. Mater. **23**, 566 (2011).

[16] T. Kato, M. Yoshio, T. Ichikawa, B. Soberats, H. Ohno, and M. Funahashi, Nat. Rev. Mater. **2**, 17001 (2017).

[17] H. Takezoe and Y. Takanishi, Jpn. J. Appl. Phys. **45**, 597 (2006).

[18] A. Seki and M. Funahashi, Chem. Lett. **45**, 616 (2016).

[19] Z. Chen, U. Baumeister, C. Tschierske, and F. Würthner, Chem. Eur. J. **13**, 450 (2007).

[20] X.-Q. Li, X. Zhang, S. Ghosh, and F. Würthner, Chem. Eur. J. **14**, 8074 (2008).

[21] T. Yasuda, H. Ooi, J. Morita, Y. Akama, K. Minoura, M. Funahashi, T. Shimomura, and T. Kato, Adv. Funct. Mater. **19**, 411 (2009).

[22] S. H. Chen, D. Katsis, A. W. Schmid, J. C. Mastrangelo, T. Tsutsuik, and T. N. Blanton, Nature (London) **397**, 506 (1999).

[23] M. Oda, H.-G. Nothofer, G. Lieser, U. Scherf, S. C. J. Meskers, and D. Neher, Adv. Mater **12**, 362 (2000).

[24] T. Hamamoto and M. Funahashi, J. Mater. Chem. C **3**, 6891 (2015).

[25] T. Sakata, M. Suzuki, T. Yamamoto, S. Nakanishi, M. Funahashi, and N. Tsurumachi, Phys. Rev. E **96**, 042704 (2017).

[26] M. Funahashi and A. Sonoda, J. Mater. Chem. **22**, 25190 (2012).

[27] R. J. Holmes and S. R. Forrest, Phys. Rev. Lett. **93**, 186404 (2004).

[28] D. G. Lidzey, D. D. C. Bradley, A. Armitage, S. Walker, and M. S. Skolnick, Science **288**, 1620 (2000).

[29] S. Kéna-Cohen, M. Davanço, and S. R. Forrest, Phys. Rev. Lett. **101**, 116401 (2008).

[30] R. Gehlhaara, R. Schüppel, M. Koschorreck, T. Fritz, H. Fröb, M. Hoffmann, V. G. Lyssenko, K. Leo, L. Connolly, J. Wenus, and D. G. Lidzey, J. Lumin. **110**, 354 (2004).